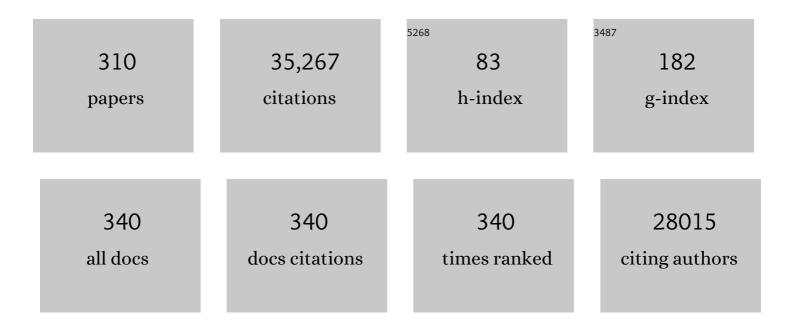
Nripan Mathews

List of Publications by Year in descending order

Source: https://exaly.com/author-pdf/112053/publications.pdf Version: 2024-02-01



#	Article	IF	CITATIONS
1	Long-Range Balanced Electron- and Hole-Transport Lengths in Organic-Inorganic CH ₃ NH ₃ Pbl ₃ . Science, 2013, 342, 344-347.	12.6	6,060
2	Low-temperature solution-processed wavelength-tunable perovskites for lasing. Nature Materials, 2014, 13, 476-480.	27.5	2,725
3	Perovskite Materials for Lightâ€Emitting Diodes and Lasers. Advanced Materials, 2016, 28, 6804-6834.	21.0	1,188
4	The origin of high efficiency in low-temperature solution-processable bilayer organometal halide hybrid solar cells. Energy and Environmental Science, 2014, 7, 399-407.	30.8	965
5	Leadâ€Free Halide Perovskite Solar Cells with High Photocurrents Realized Through Vacancy Modulation. Advanced Materials, 2014, 26, 7122-7127.	21.0	942
6	Lead-free germanium iodide perovskite materials for photovoltaic applications. Journal of Materials Chemistry A, 2015, 3, 23829-23832.	10.3	841
7	Advancements in perovskite solar cells: photophysics behind the photovoltaics. Energy and Environmental Science, 2014, 7, 2518-2534.	30.8	694
8	Formamidinium-Containing Metal-Halide: An Alternative Material for Near-IR Absorption Perovskite Solar Cells. Journal of Physical Chemistry C, 2014, 118, 16458-16462.	3.1	657
9	Flexible, low-temperature, solution processed ZnO-based perovskite solid state solar cells. Chemical Communications, 2013, 49, 11089.	4.1	553
10	Synthesis of porous NiO nanocrystals with controllable surface area and their application as supercapacitor electrodes. Nano Research, 2010, 3, 643-652.	10.4	534
11	Band-gap tuning of lead halide perovskites using a sequential deposition process. Journal of Materials Chemistry A, 2014, 2, 9221-9225.	10.3	494
12	Inorganic Halide Perovskites for Efficient Light-Emitting Diodes. Journal of Physical Chemistry Letters, 2015, 6, 4360-4364.	4.6	482
13	Lead-Free MA ₂ CuCl _{<i>x</i>} Br _{4–<i>x</i>} Hybrid Perovskites. Inorganic Chemistry, 2016, 55, 1044-1052.	4.0	457
14	Formamidinium tin-based perovskite with low E _g for photovoltaic applications. Journal of Materials Chemistry A, 2015, 3, 14996-15000.	10.3	449
15	Laminated Carbon Nanotube Networks for Metal Electrode-Free Efficient Perovskite Solar Cells. ACS Nano, 2014, 8, 6797-6804.	14.6	427
16	Ultrathin films on copper(i) oxide water splitting photocathodes: a study on performance and stability. Energy and Environmental Science, 2012, 5, 8673.	30.8	401
17	Current progress and future perspectives for organic/inorganic perovskite solar cells. Materials Today, 2014, 17, 16-23.	14.2	349
18	Surface Recombination and Collection Efficiency in Perovskite Solar Cells from Impedance Analysis. Journal of Physical Chemistry Letters, 2016, 7, 5105-5113.	4.6	346

#	Article	IF	CITATIONS
19	Impact of Anionic Br [–] Substitution on Open Circuit Voltage in Lead Free Perovskite (CsSnI _{3-x} Br _{<i>x</i>}) Solar Cells. Journal of Physical Chemistry C, 2015, 119, 1763-1767.	3.1	332
20	Slow cooling and highly efficient extraction of hot carriers in colloidal perovskite nanocrystals. Nature Communications, 2017, 8, 14350.	12.8	282
21	Enhancement in the Performance of Ultrathin Hematite Photoanode for Water Splitting by an Oxide Underlayer. Advanced Materials, 2012, 24, 2699-2702.	21.0	271
22	Discerning the Surface and Bulk Recombination Kinetics of Organic–Inorganic Halide Perovskite Single Crystals. Advanced Energy Materials, 2016, 6, 1600551.	19.5	271
23	Perovskite Solar Cells: Beyond Methylammonium Lead Iodide. Journal of Physical Chemistry Letters, 2015, 6, 898-907.	4.6	266
24	Synergistic Gating of Electroâ€lonoâ€Photoactive 2D Chalcogenide Neuristors: Coexistence of Hebbian and Homeostatic Synaptic Metaplasticity. Advanced Materials, 2018, 30, e1800220.	21.0	261
25	Highly Efficient Thermally Co-evaporated Perovskite Solar Cells and Mini-modules. Joule, 2020, 4, 1035-1053.	24.0	257
26	Nanostructuring Mixedâ€Dimensional Perovskites: A Route Toward Tunable, Efficient Photovoltaics. Advanced Materials, 2016, 28, 3653-3661.	21.0	251
27	Perovskite–Hematite Tandem Cells for Efficient Overall Solar Driven Water Splitting. Nano Letters, 2015, 15, 3833-3839.	9.1	249
28	Rb as an Alternative Cation for Templating Inorganic Lead-Free Perovskites for Solution Processed Photovoltaics. Chemistry of Materials, 2016, 28, 7496-7504.	6.7	249
29	A Photonic Crystal Laser from Solution Based Organo-Lead Iodide Perovskite Thin Films. ACS Nano, 2016, 10, 3959-3967.	14.6	238
30	Solutionâ€Processed Tinâ€Based Perovskite for Nearâ€Infrared Lasing. Advanced Materials, 2016, 28, 8191-8196.	21.0	222
31	Charge Accumulation and Hysteresis in Perovskiteâ€Based Solar Cells: An Electroâ€Optical Analysis. Advanced Energy Materials, 2015, 5, 1500829.	19.5	217
32	Computational Study of Halide Perovskite-Derived A ₂ BX ₆ Inorganic Compounds: Chemical Trends in Electronic Structure and Structural Stability. Chemistry of Materials, 2017, 29, 7740-7749.	6.7	215
33	A large area (70 cm ²) monolithic perovskite solar module with a high efficiency and stability. Energy and Environmental Science, 2016, 9, 3687-3692.	30.8	213
34	Hydrothermal Synthesis of High Electron Mobility Zn-doped SnO ₂ Nanoflowers as Photoanode Material for Efficient Dye-Sensitized Solar Cells. Chemistry of Materials, 2011, 23, 3938-3945.	6.7	206
35	Morphology-Independent Stable White-Light Emission from Self-Assembled Two-Dimensional Perovskites Driven by Strong Exciton–Phonon Coupling to the Organic Framework. Chemistry of Materials, 2017, 29, 3947-3953.	6.7	200
36	Interfacial Electron Transfer Barrier at Compact TiO ₂ /CH ₃ NH ₃ PbI ₃ Heterojunction. Small, 2015, 11, 3606-3613.	10.0	196

#	Article	IF	CITATIONS
37	Polaron self-localization in white-light emitting hybrid perovskites. Journal of Materials Chemistry C, 2017, 5, 2771-2780.	5.5	196
38	Rutile TiO2-based perovskite solar cells. Journal of Materials Chemistry A, 2014, 2, 9251.	10.3	188
39	Rational Design: A High-Throughput Computational Screening and Experimental Validation Methodology for Lead-Free and Emergent Hybrid Perovskites. ACS Energy Letters, 2017, 2, 837-845.	17.4	187
40	High efficiency electrospun TiO ₂ nanofiber based hybrid organic–inorganic perovskite solar cell. Nanoscale, 2014, 6, 1675-1679.	5.6	185
41	Highly Spin-Polarized Carrier Dynamics and Ultralarge Photoinduced Magnetization in CH ₃ NH ₃ Pbl ₃ Perovskite Thin Films. Nano Letters, 2015, 15, 1553-1558.	9.1	183
42	Giant five-photon absorption from multidimensional core-shell halide perovskite colloidal nanocrystals. Nature Communications, 2017, 8, 15198.	12.8	177
43	A swivel-cruciform thiophene based hole-transporting material for efficient perovskite solar cells. Journal of Materials Chemistry A, 2014, 2, 6305-6309.	10.3	167
44	Enhancing moisture tolerance in efficient hybrid 3D/2D perovskite photovoltaics. Journal of Materials Chemistry A, 2018, 6, 2122-2128.	10.3	163
45	Spectral Features and Charge Dynamics of Lead Halide Perovskites: Origins and Interpretations. Accounts of Chemical Research, 2016, 49, 294-302.	15.6	159
46	Flexible Ionicâ€Electronic Hybrid Oxide Synaptic TFTs with Programmable Dynamic Plasticity for Brainâ€Inspired Neuromorphic Computing. Small, 2017, 13, 1701193.	10.0	152
47	Ionotronic Halide Perovskite Driftâ€Diffusive Synapses for Lowâ€Power Neuromorphic Computation. Advanced Materials, 2018, 30, e1805454.	21.0	146
48	Characteristics of the Electrical Percolation in Carbon Nanotubes/Polymer Nanocomposites. Journal of Physical Chemistry C, 2011, 115, 21685-21690.	3.1	142
49	Interfacial Charge Transfer Anisotropy in Polycrystalline Lead Iodide Perovskite Films. Journal of Physical Chemistry Letters, 2015, 6, 1396-1402.	4.6	141
50	CdSe-sensitized mesoscopic TiO2 solar cells exhibiting >5% efficiency: redundancy of CdS buffer layer. Journal of Materials Chemistry, 2012, 22, 16235.	6.7	140
51	Iron Pyrite Thin Film Counter Electrodes for Dye-Sensitized Solar Cells: High Efficiency for Iodine and Cobalt Redox Electrolyte Cells. ACS Nano, 2014, 8, 10597-10605.	14.6	138
52	Highly stable, luminescent core–shell type methylammonium–octylammonium lead bromide layered perovskite nanoparticles. Chemical Communications, 2016, 52, 7118-7121.	4.1	138
53	Over 20% Efficient CIGS–Perovskite Tandem Solar Cells. ACS Energy Letters, 2017, 2, 807-812.	17.4	135
54	Self-assembled hierarchical nanostructured perovskites enable highly efficient LEDs <i>via</i> an energy cascade. Energy and Environmental Science, 2018, 11, 1770-1778.	30.8	135

#	Article	IF	CITATIONS
55	Towards printable organic thin film transistor based flash memory devices. Journal of Materials Chemistry, 2011, 21, 5203.	6.7	133
56	In situ photo-assisted deposition of MoS2 electrocatalyst onto zinc cadmium sulphide nanoparticle surfaces to construct an efficient photocatalyst for hydrogen generation. Nanoscale, 2013, 5, 1479.	5.6	133
57	Limitations of Cs ₃ Bi ₂ I ₉ as Lead-Free Photovoltaic Absorber Materials. ACS Applied Materials & Interfaces, 2018, 10, 35000-35007.	8.0	133
58	Effect of Cation Composition on the Mechanical Stability of Perovskite Solar Cells. Advanced Energy Materials, 2018, 8, 1702116.	19.5	130
59	Identifying Fundamental Limitations in Halide Perovskite Solar Cells. Advanced Materials, 2016, 28, 2439-2445.	21.0	129
60	On the Solar to Hydrogen Conversion Efficiency of Photoelectrodes for Water Splitting. Journal of Physical Chemistry Letters, 2014, 5, 3330-3334.	4.6	128
61	Transparent, Conducting Nb:SnO ₂ for Host–Guest Photoelectrochemistry. Nano Letters, 2012, 12, 5431-5435.	9.1	122
62	Solution processed transition metal sulfides: application as counter electrodes in dye sensitized solar cells (DSCs). Physical Chemistry Chemical Physics, 2011, 13, 19307.	2.8	121
63	Poor Photovoltaic Performance of Cs ₃ Bi ₂ I ₉ : An Insight through First-Principles Calculations. Journal of Physical Chemistry C, 2017, 121, 17062-17067.	3.1	121
64	Uncovering loss mechanisms in silver nanoparticle-blended plasmonic organic solar cells. Nature Communications, 2013, 4, 2004.	12.8	118
65	Ultrathin MnO2 nanoflakes as efficient catalysts for oxygen reduction reaction. Chemical Communications, 2014, 50, 7885.	4.1	113
66	Tunable room-temperature spin-selective optical Stark effect in solution-processed layered halide perovskites. Science Advances, 2016, 2, e1600477.	10.3	112
67	Cesium Copper Iodide Tailored Nanoplates and Nanorods for Blue, Yellow, and White Emission. Chemistry of Materials, 2019, 31, 9003-9011.	6.7	111
68	Low threshold and efficient multiple exciton generation in halide perovskite nanocrystals. Nature Communications, 2018, 9, 4197.	12.8	110
69	Halide perovskite memristors as flexible and reconfigurable physical unclonable functions. Nature Communications, 2021, 12, 3681.	12.8	107
70	Spinel Co ₃ O ₄ nanomaterials for efficient and stable large area carbon-based printed perovskite solar cells. Nanoscale, 2018, 10, 2341-2350.	5.6	106
71	High-throughput Computational Study of Halide Double Perovskite Inorganic Compounds. Chemistry of Materials, 2019, 31, 5392-5401.	6.7	102
72	Enhanced Exciton and Photon Confinement in Ruddlesden–Popper Perovskite Microplatelets for Highly Stable Lowâ€Threshold Polarized Lasing. Advanced Materials, 2018, 30, e1707235.	21.0	101

#	Article	IF	CITATIONS
73	Benzyl Alcohol-Treated CH ₃ NH ₃ PbBr ₃ Nanocrystals Exhibiting High Luminescence, Stability, and Ultralow Amplified Spontaneous Emission Thresholds. Nano Letters, 2017, 17, 7424-7432.	9.1	100
74	Micellar poly(styrene-b-4-vinylpyridine)-nanoparticle hybrid system for non-volatile organic transistor memory. Journal of Materials Chemistry, 2009, 19, 7354.	6.7	99
75	Efficient multispectral photodetection using Mn doped ZnO nanowires. Journal of Materials Chemistry, 2012, 22, 9678.	6.7	97
76	Unravelling the Effects of Cl Addition in Single Step CH ₃ NH ₃ Pbl ₃ Perovskite Solar Cells. Chemistry of Materials, 2015, 27, 2309-2314.	6.7	96
77	Hybrid graphene–metal nanoparticle systems: electronic properties and gas interaction. Journal of Materials Chemistry, 2011, 21, 15593.	6.7	94
78	Si photocathode with Ag-supported dendritic Cu catalyst for CO ₂ reduction. Energy and Environmental Science, 2019, 12, 1068-1077.	30.8	93
79	Crown Ethers Enable Room-Temperature Synthesis of CsPbBr ₃ Quantum Dots for Light-Emitting Diodes. ACS Energy Letters, 2018, 3, 526-531.	17.4	92
80	One‣tep Inkjet Printed Perovskite in Air for Efficient Light Harvesting. Solar Rrl, 2018, 2, 1700217.	5.8	90
81	Multidimensional Perovskites: A Mixed Cation Approach Towards Ambient Stable and Tunable Perovskite Photovoltaics. ChemSusChem, 2016, 9, 2541-2558.	6.8	88
82	Carbon nanotubes as an efficient hole collector for high voltage methylammonium lead bromide perovskite solar cells. Nanoscale, 2016, 8, 6352-6360.	5.6	88
83	Indirect tail states formation by thermal-induced polar fluctuations in halide perovskites. Nature Communications, 2019, 10, 484.	12.8	88
84	Facile Photochemical Synthesis of Graphene-Pt Nanoparticle Composite for Counter Electrode in Dye Sensitized Solar Cell. ACS Applied Materials & Interfaces, 2012, 4, 3447-3452.	8.0	85
85	Highly efficient Cs-based perovskite light-emitting diodes enabled by energy funnelling. Chemical Communications, 2017, 53, 12004-12007.	4.1	85
86	Designing Efficient Energy Funneling Kinetics in Ruddlesden–Popper Perovskites for Highâ€Performance Lightâ€Emitting Diodes. Advanced Materials, 2018, 30, e1800818.	21.0	85
87	Superior Performance of Silver Bismuth Iodide Photovoltaics Fabricated via Dynamic Hotâ€Casting Method under Ambient Conditions. Advanced Energy Materials, 2018, 8, 1802051.	19.5	84
88	Effect of the Ionic Conductivity on the Performance of Polyelectrolyteâ€Based Supercapacitors. Advanced Functional Materials, 2010, 20, 4344-4350.	14.9	83
89	Diffusive and Drift Halide Perovskite Memristive Barristors as Nociceptive and Synaptic Emulators for Neuromorphic Computing. Advanced Materials, 2021, 33, 2007851.	21.0	83
90	Energy level alignment at the methylammonium lead iodide/copper phthalocyanine interface. APL Materials, 2014, 2, .	5.1	80

#	Article	IF	CITATIONS
91	Completely Solvent-free Protocols to Access Phase-Pure, Metastable Metal Halide Perovskites and Functional Photodetectors from the Precursor Salts. IScience, 2019, 16, 312-325.	4.1	80
92	Bifacial, Color-Tunable Semitransparent Perovskite Solar Cells for Building-Integrated Photovoltaics. ACS Applied Materials & Interfaces, 2020, 12, 484-493.	8.0	80
93	Synthesis of gold nanoshells based on the depositionprecipitation process. Gold Bulletin, 2008, 41, 23-36.	2.7	78
94	Perovskite Nanoparticles: Synthesis, Properties, and Novel Applications in Photovoltaics and LEDs. Small Methods, 2019, 3, 1800231.	8.6	77
95	Incorporation of Cl into sequentially deposited lead halide perovskite films for highly efficient mesoporous solar cells. Nanoscale, 2014, 6, 13854-13860.	5.6	76
96	Novel Plasma-Assisted Low-Temperature-Processed SnO ₂ Thin Films for Efficient Flexible Perovskite Photovoltaics. ACS Energy Letters, 2018, 3, 1482-1491.	17.4	75
97	Dominant factors limiting the optical gain in layered two-dimensional halide perovskite thin films. Physical Chemistry Chemical Physics, 2016, 18, 14701-14708.	2.8	73
98	Broadbandâ€Emitting 2 D Hybrid Organic–Inorganic Perovskite Based on Cyclohexaneâ€bis(methylamonium) Cation. ChemSusChem, 2017, 10, 3765-3772.	6.8	72
99	Directed Assembly of Liquid Metal–Elastomer Conductors for Stretchable and Selfâ€Healing Electronics. Advanced Materials, 2020, 32, e2001642.	21.0	72
100	Facile Method to Reduce Surface Defects and Trap Densities in Perovskite Photovoltaics. ACS Applied Materials & Interfaces, 2017, 9, 21292-21297.	8.0	71
101	Atomically Altered Hematite for Highly Efficient Perovskite Tandem Waterâ€Splitting Devices. ChemSusChem, 2017, 10, 2449-2456.	6.8	71
102	Additive Selection Strategy for High Performance Perovskite Photovoltaics. Journal of Physical Chemistry C, 2018, 122, 13884-13893.	3.1	71
103	Highly Efficient Semitransparent Perovskite Solar Cells for Four Terminal Perovskite-Silicon Tandems. ACS Applied Materials & Interfaces, 2019, 11, 34178-34187.	8.0	71
104	Designing the Perovskite Structural Landscape for Efficient Blue Emission. ACS Energy Letters, 2020, 5, 1593-1600.	17.4	71
105	Ultralow Power Dual-Gated Subthreshold Oxide Neuristors: An Enabler for Higher Order Neuronal Temporal Correlations. ACS Nano, 2018, 12, 11263-11273.	14.6	70
106	Ultrafine Gold Nanowire Networks as Plasmonic Antennae in Organic Photovoltaics. Journal of Physical Chemistry C, 2012, 116, 6453-6458.	3.1	69
107	Self-assembly of a robust hydrogen-bonded octylphosphonate network on cesium lead bromide perovskite nanocrystals for light-emitting diodes. Nanoscale, 2019, 11, 12370-12380.	5.6	67
108	Coherent Spin and Quasiparticle Dynamics in Solutionâ€Processed Layered 2D Lead Halide Perovskites. Advanced Science, 2018, 5, 1800664.	11.2	66

#	Article	IF	CITATIONS
109	Loading of mesoporous titania films by CH ₃ NH ₃ PbI ₃ perovskite, single step <i>vs.</i> sequential deposition. Chemical Communications, 2015, 51, 4603-4606.	4.1	64
110	Al ₂ O ₃ Surface Complexation for Photocatalytic Organic Transformations. Journal of the American Chemical Society, 2017, 139, 269-276.	13.7	64
111	Lead Halide Perovskite Nanocrystals: Room Temperature Syntheses toward Commercial Viability. Advanced Energy Materials, 2020, 10, 2001349.	19.5	63
112	Self healable neuromorphic memtransistor elements for decentralized sensory signal processing in robotics. Nature Communications, 2020, 11, 4030.	12.8	63
113	Low-Temperature Chemical Transformations for High-Performance Solution-Processed Oxide Transistors. Chemistry of Materials, 2016, 28, 8305-8313.	6.7	61
114	Recovery of Shallow Charge-Trapping Defects in CsPbX ₃ Nanocrystals through Specific Binding and Encapsulation with Amino-Functionalized Silanes. ACS Energy Letters, 2018, 3, 1409-1414.	17.4	60
115	Organic neuromorphic devices: Past, present, and future challenges. MRS Bulletin, 2020, 45, 619-630.	3.5	59
116	Oxide nanowire networks and their electronic and optoelectronic characteristics. Nanoscale, 2010, 2, 1984.	5.6	58
117	Zinc Tin Oxide (ZTO) electron transporting buffer layer in inverted organic solar cell. Organic Electronics, 2012, 13, 870-874.	2.6	58
118	Transparent Flexible Multifunctional Nanostructured Architectures for Non-optical Readout, Proximity, and Pressure Sensing. ACS Applied Materials & Interfaces, 2017, 9, 15015-15021.	8.0	58
119	Cu-doped nickel oxide interface layer with nanoscale thickness for efficient and highly stable printable carbon-based perovskite solar cell. Solar Energy, 2019, 182, 225-236.	6.1	58
120	Tuning Electrical Properties in Amorphous Zinc Tin Oxide Thin Films for Solution Processed Electronics. ACS Applied Materials & amp; Interfaces, 2014, 6, 773-777.	8.0	56
121	Origin of Photocarrier Losses in Iron Pyrite (FeS ₂) Nanocubes. ACS Nano, 2016, 10, 4431-4440.	14.6	56
122	Hot carrier extraction in CH ₃ NH ₃ PbI ₃ unveiled by pump-push-probe spectroscopy. Science Advances, 2019, 5, eaax3620.	10.3	56
123	2D black phosphorous nanosheets as a hole transporting material in perovskite solar cells. Journal of Power Sources, 2017, 371, 156-161.	7.8	52
124	High- <i>k</i> , Ultrastretchable Self-Enclosed Ionic Liquid-Elastomer Composites for Soft Robotics and Flexible Electronics. ACS Applied Materials & amp; Interfaces, 2020, 12, 37561-37570.	8.0	51
125	Light scattering enhancement from sub-micrometer cavities in the photoanode for dye-sensitized solar cells. Journal of Materials Chemistry, 2012, 22, 16201.	6.7	50
126	Cobalt Dopant with Deep Redox Potential for Organometal Halide Hybrid Solar Cells. ChemSusChem, 2014, 7, 1909-1914.	6.8	50

#	Article	IF	CITATIONS
127	Realizing Reduced Imperfections via Quantum Dots Interdiffusion in High Efficiency Perovskite Solar Cells. Advanced Materials, 2020, 32, e2003296.	21.0	50
128	Band engineered ternary solid solution CdSxSe1â^'x-sensitized mesoscopic TiO2 solar cells. Physical Chemistry Chemical Physics, 2012, 14, 7154.	2.8	47
129	Efficiency Enhancement in Bulk-Heterojunction Solar Cells Integrated with Large-Area Ag Nanotriangle Arrays. Journal of Physical Chemistry C, 2012, 116, 14820-14825.	3.1	46
130	Evolution of hydrogen by few-layered black phosphorus under visible illumination. Journal of Materials Chemistry A, 2017, 5, 24874-24879.	10.3	45
131	Aligned Tin Oxide Nanonets for High-Performance Transistors. Journal of Physical Chemistry C, 2010, 114, 1331-1336.	3.1	44
132	Extended Absorption Window and Improved Stability of Cesium-Based Triple-Cation Perovskite Solar Cells Passivated with Perfluorinated Organics. ACS Energy Letters, 2018, 3, 1068-1076.	17.4	44
133	Influence of 4-tert-Butylpyridine in DSCs with Coll/III Redox Mediator. Journal of Physical Chemistry C, 2013, 117, 15515-15522.	3.1	42
134	Metal Coordination Sphere Deformation Induced Highly Stokesâ€Shifted, Ultra Broadband Emission in 2D Hybrid Leadâ€Bromide Perovskites and Investigation of Its Origin. Angewandte Chemie - International Edition, 2020, 59, 10791-10796.	13.8	42
135	Stabilizing the Electroluminescence of Halide Perovskites with Potassium Passivation. ACS Energy Letters, 2020, 5, 1804-1813.	17.4	41
136	Hot Carriers in Halide Perovskites: How Hot Truly?. Journal of Physical Chemistry Letters, 2020, 11, 2743-2750.	4.6	41
137	Inducing formation of a corrugated, white-light emitting 2D lead-bromide perovskite <i>via</i> subtle changes in templating cation. Journal of Materials Chemistry C, 2020, 8, 889-893.	5.5	40
138	Enabling high performance n-type metal oxide semiconductors at low temperatures for thin film transistors. Inorganic Chemistry Frontiers, 2020, 7, 1822-1844.	6.0	40
139	Precise Control of CsPbBr ₃ Perovskite Nanocrystal Growth at Room Temperature: Size Tunability and Synthetic Insights. Chemistry of Materials, 2021, 33, 2387-2397.	6.7	40
140	Coâ€Evaporated MAPbI ₃ with Graded Fermi Levels Enables Highly Performing, Scalable, and Flexible pâ€iâ€n Perovskite Solar Cells. Advanced Functional Materials, 2021, 31, 2103252.	14.9	40
141	Mixed-Dimensional Naphthylmethylammonium-Methylammonium Lead Iodide Perovskites with Improved Thermal Stability. Scientific Reports, 2020, 10, 429.	3.3	39
142	Colorful Perovskite Solar Cells: Progress, Strategies, and Potentials. Journal of Physical Chemistry Letters, 2021, 12, 1321-1329.	4.6	39
143	Alkali Additives Enable Efficient Large Area (>55 cm ²) Slotâ€Đie Coated Perovskite Solar Modules. Advanced Functional Materials, 2022, 32, .	14.9	39
144	Improving Photocatalytic H ₂ Evolution of TiO ₂ via Formation of {001}–{010} Quasi-Heterojunctions. Journal of Physical Chemistry C, 2013, 117, 22894-22902.	3.1	38

#	Article	IF	CITATIONS
145	Indium Tungsten Oxide Thin Films for Flexible High-Performance Transistors and Neuromorphic Electronics. ACS Applied Materials & Interfaces, 2018, 10, 30506-30513.	8.0	38
146	Ultrafast long-range spin-funneling in solution-processed Ruddlesden–Popper halide perovskites. Nature Communications, 2019, 10, 3456.	12.8	38
147	Halide Perovskite Quantum Dots Photosensitizedâ€Amorphous Oxide Transistors for Multimodal Synapses. Advanced Materials Technologies, 2020, 5, 2000514.	5.8	38
148	Halide Perovskite Solar Cells for Building Integrated Photovoltaics: Transforming Building Façades into Power Generators. Advanced Materials, 2022, 34, e2104661.	21.0	37
149	Facile synthesis of a hole transporting material with a silafluorene core for efficient mesoscopic CH ₃ NH ₃ PbI ₃ perovskite solar cells. Journal of Materials Chemistry A, 2016, 4, 8750-8754.	10.3	36
150	Healable and flexible transparent heaters. Nanoscale, 2017, 9, 14990-14997.	5.6	36
151	Improved photovoltaic performance of triple-cation mixed-halide perovskite solar cells with binary trivalent metals incorporated into the titanium dioxide electron transport layer. Journal of Materials Chemistry C, 2019, 7, 5028-5036.	5.5	36
152	Optogenetics inspired transition metal dichalcogenide neuristors for in-memory deep recurrent neural networks. Nature Communications, 2020, 11, 3211.	12.8	36
153	Excellent Intrinsic Longâ€Term Thermal Stability of Coâ€Evaporated MAPbI ₃ Solar Cells at 85 °C. Advanced Functional Materials, 2021, 31, 2100557.	14.9	36
154	Solution processed non-volatile top-gate polymer field-effect transistors. Journal of Materials Chemistry, 2011, 21, 8971.	6.7	34
155	Uncovering alternate charge transfer mechanisms in Escherichia coli chemically functionalized with conjugated oligoelectrolytes. Chemical Communications, 2014, 50, 8223-8226.	4.1	34
156	Cubic NaSbS ₂ as an Ionic–Electronic Coupled Semiconductor for Switchable Photovoltaic and Neuromorphic Device Applications. Advanced Materials, 2020, 32, e1906976.	21.0	34
157	Elucidating the Localized Plasmonic Enhancement Effects from a Single Ag Nanowire in Organic Solar Cells. ACS Nano, 2014, 8, 10101-10110.	14.6	33
158	Modulating carrier dynamics through perovskite film engineering. Physical Chemistry Chemical Physics, 2016, 18, 27119-27123.	2.8	33
159	Role of Water in Suppressing Recombination Pathways in CH ₃ NH ₃ PbI ₃ Perovskite Solar Cells. ACS Applied Materials & Interfaces, 2019, 11, 25474-25482.	8.0	33
160	Effect of TiO ₂ Mesoporous Layer and Surface Treatments in Determining Efficiencies in Antimony Sulfide-(Sb ₂ S ₃) Sensitized Solar Cells. Journal of the Electrochemical Society, 2012, 159, B247-B250.	2.9	32
161	Ruddlesden-Popper Perovskite Solar Cells. CheM, 2017, 2, 326-327.	11.7	31
162	Simplified Architecture of a Fully Printable Perovskite Solar Cell Using a Thick Zirconia Layer. Energy Technology, 2017, 5, 1866-1872.	3.8	31

#	Article	IF	CITATIONS
163	Highly Transparent and Integrable Surface Texture Change Device for Localized Tactile Feedback. Small, 2018, 14, 1702312.	10.0	31
164	Broadband emission from zero-dimensional Cs ₄ PbI ₆ perovskite nanocrystals. RSC Advances, 2020, 10, 13431-13436.	3.6	31
165	Effect of Excess PbI ₂ in Fully Printable Carbonâ€based Perovskite Solar Cells. Energy Technology, 2017, 5, 1880-1886.	3.8	30
166	Doping and Switchable Photovoltaic Effect in Leadâ€Free Perovskites Enabled by Metal Cation Transmutation. Advanced Materials, 2018, 30, e1802080.	21.0	30
167	Cesium Lead Halide Perovskite Nanocrystals Prepared by Anion Exchange for Light-Emitting Diodes. ACS Applied Nano Materials, 2020, 3, 1766-1774.	5.0	30
168	Facile One-Step Synthesis of CdS _{<i>x</i>} Se _{1–<i>x</i>} Nanobelts with Uniform and Controllable Stoichiometry. Journal of Physical Chemistry C, 2011, 115, 19538-19545.	3.1	29
169	A high voltage solar cell using a donor–acceptor conjugated polymer based on pyrrolo[3,4-f]-2,1,3-benzothiadiazole-5,7-dione. Journal of Materials Chemistry A, 2014, 2, 17925-17933.	10.3	29
170	Design of Perovskite Thermally Coâ€Evaporated Highly Efficient Miniâ€Modules with High Geometrical Fill Factors. Solar Rrl, 2020, 4, 2000473.	5.8	29
171	Soft Actuator Materials for Electrically Driven Haptic Interfaces. Advanced Intelligent Systems, 2022, 4, 2100061.	6.1	29
172	Influence of void-free perovskite capping layer on the charge recombination process in high performance CH ₃ NH ₃ PbI ₃ perovskite solar cells. Nanoscale, 2016, 8, 4181-4193.	5.6	28
173	Rapid Crystallization of All-Inorganic CsPbBr3 Perovskite for High-Brightness Light-Emitting Diodes. ACS Omega, 2017, 2, 2757-2764.	3.5	28
174	Reversible Electrochemical Silver Deposition over Large Areas for Smart Windows and Information Display. Electrochimica Acta, 2017, 255, 63-71.	5.2	28
175	Effect of Formamidinium/Cesium Substitution and Pbl ₂ on the Longâ€Term Stability of Tripleâ€Cation Perovskites. ChemSusChem, 2017, 10, 3804-3809.	6.8	28
176	Localized Traps Limited Recombination in Lead Bromide Perovskites. Advanced Energy Materials, 2019, 9, 1803119.	19.5	28
177	Investigating the structure–function relationship in triple cation perovskite nanocrystals for light-emitting diode applications. Journal of Materials Chemistry C, 2020, 8, 11805-11821.	5.5	27
178	Temperature and Electrical Poling Effects on Ionic Motion in MAPbI ₃ Photovoltaic Cells. Advanced Energy Materials, 2017, 7, 1700265.	19.5	26
179	A rapid low temperature self-healable polymeric composite for flexible electronic devices. Journal of Materials Chemistry A, 2018, 6, 21428-21434.	10.3	26
180	Perovskite nanostructures: Leveraging quantum effects to challenge optoelectronic limits. Materials Today, 2020, 33, 122-140.	14.2	26

#	Article	IF	CITATIONS
181	Targeted Synthesis of Trimeric Organic–Bromoplumbate Hybrids That Display Intrinsic, Highly Stokes-Shifted, Broadband Emission. Chemistry of Materials, 2020, 32, 4431-4441.	6.7	25
182	Deterministic Light Yield, Fast Scintillation, and Microcolumn Structures in Lead Halide Perovskite Nanocrystals. Journal of Physical Chemistry C, 2021, 125, 14082-14088.	3.1	25
183	Advances and Potentials of NiO _{<i>x</i>} Surface Treatments for pâ^iâ^in Perovskite Solar Cells. Solar Rrl, 2022, 6, 2100700.	5.8	25
184	Upcycling Silicon Photovoltaic Waste into Thermoelectrics. Advanced Materials, 2022, 34, e2110518.	21.0	25
185	Modulating Cationic Ratios for High-Performance Transparent Solution-Processed Electronics. ACS Applied Materials & Interfaces, 2016, 8, 1139-1146.	8.0	24
186	Design of 2D Templating Molecules for Mixed-Dimensional Perovskite Light-Emitting Diodes. Chemistry of Materials, 2020, 32, 8097-8105.	6.7	24
187	Direct Band Gap Mixed-Valence Organic–inorganic Gold Perovskite as Visible Light Absorbers. Chemistry of Materials, 2020, 32, 6318-6325.	6.7	24
188	Adaptive Latent Inhibition in Associatively Responsive Optoelectronic Synapse. Advanced Functional Materials, 2021, 31, 2100807.	14.9	24
189	Additives in Halide Perovskite for Blue-Light-Emitting Diodes: Passivating Agents or Crystallization Modulators?. ACS Energy Letters, 2021, 6, 4265-4272.	17.4	24
190	The role of tin oxide surface defects in determining nanonet FET response to humidity and photoexcitation. Journal of Materials Chemistry C, 2014, 2, 940-945.	5.5	23
191	Highly stable and efficient planar perovskite solar cells using ternary metal oxide electron transport layers. Journal of Power Sources, 2020, 448, 227362.	7.8	23
192	Controlling the film structure by regulating 2D Ruddlesden–Popper perovskite formation enthalpy for efficient and stable tri-cation perovskite solar cells. Journal of Materials Chemistry A, 2020, 8, 5874-5881.	10.3	23
193	Reversible Photochromism in ⟠110⟩ Oriented Layered Halide Perovskite. ACS Nano, 2022, 16, 2942-2952.	14.6	23
194	Resonant Aluminum Nanodisk Array for Enhanced Tunable Broadband Light Trapping in Ultrathin Bulk Heterojunction Organic Photovoltaic Devices. Plasmonics, 2012, 7, 677-684.	3.4	22
195	Paper like free-standing hybrid single-walled carbon nanotubes air electrodes for zinc–air batteries. Journal of Solid State Electrochemistry, 2012, 16, 1585-1593.	2.5	22
196	Highly Active MnO Catalysts Integrated onto Fe ₂ O ₃ Nanorods for Efficient Water Splitting. Advanced Materials Interfaces, 2016, 3, 1600176.	3.7	22
197	The Physics of Interlayer Exciton Delocalization in Ruddlesden–Popper Lead Halide Perovskites. Nano Letters, 2021, 21, 405-413.	9.1	22
198	Evolution of Perovskite Crystallization in Printed Mesoscopic Perovskite Solar Cells. Energy Technology, 2019, 7, 1900343.	3.8	21

#	Article	IF	CITATIONS
199	Stable Sn ²⁺ doped FAPbl ₃ nanocrystals for near-infrared LEDs. Chemical Communications, 2019, 55, 5451-5454.	4.1	21
200	Hybrid organic–inorganic halide perovskites for scaled-in neuromorphic devices. MRS Bulletin, 2020, 45, 641-648.	3.5	21
201	White Electroluminescence from Perovskite–Organic Heterojunction. ACS Energy Letters, 2020, 5, 2690-2697.	17.4	21
202	Printing materials for electronic devices. International Journal of Materials Research, 2010, 101, 236-250.	0.3	20
203	Photovoltage enhancement from cyanobiphenyl liquid crystals and 4-tert-butylpyridine in Co(ii/iii) mediated dye-sensitized solar cells. Chemical Communications, 2013, 49, 9101.	4.1	20
204	Reducing Massâ€Transport Limitations in Cobaltâ€Electrolyteâ€Based Dyeâ€Sensitized Solar Cells by Photoanode Modification. ChemPhysChem, 2014, 15, 1216-1221.	2.1	20
205	High Stability Bilayered Perovskites through Crystallization Driven Self-Assembly. ACS Applied Materials & Interfaces, 2017, 9, 28743-28749.	8.0	20
206	Room temperature synthesis of low-dimensional rubidium copper halide colloidal nanocrystals with near unity photoluminescence quantum yield. Nanoscale, 2021, 13, 59-65.	5.6	20
207	Facile fabrication of graphene devices through metalloporphyrin induced photocatalytic reduction. RSC Advances, 2012, 2, 4120.	3.6	19
208	Investigating the feasibility of symmetric guanidinium based plumbate perovskites in prototype solar cell devices. Japanese Journal of Applied Physics, 2017, 56, 08MC05.	1.5	19
209	Unveiling the role of carbon black in printable mesoscopic perovskite solar cells. Journal of Power Sources, 2021, 501, 230019.	7.8	19
210	High-surface-area, interconnected, nanofibrillar TiO2 structures as photoanodes in dye-sensitized solar cells. Scripta Materialia, 2013, 68, 487-490.	5.2	18
211	Hybrid 2D [Pb(CH ₃ NH ₂)I ₂] _{<i>n</i>} Coordination Polymer Precursor for Scalable Perovskite Deposition. ACS Energy Letters, 2020, 5, 2305-2312.	17.4	18
212	Formation of Corrugated <i>n</i> = 1 2D Tin lodide Perovskites and Their Use as Lead-Free Solar Absorbers. ACS Nano, 2021, 15, 6395-6409.	14.6	18
213	Zn-Doped SnO ₂ Nanocrystals as Efficient DSSC Photoanode Material and Remarkable Photocurrent Enhancement by Interface Modification. Journal of the Electrochemical Society, 2012, 159, H735-H739.	2.9	17
214	Nitrogen doped cuprous oxide as low cost hole-transporting material for perovskite solar cells. Scripta Materialia, 2018, 153, 104-108.	5.2	16
215	Effects of energetics with {001} facet-dominant anatase TiO2 scaffold on electron transport in CH3NH3PbI3 perovskite solar cells. Electrochimica Acta, 2019, 300, 445-454.	5.2	16
216	Lowâ€Temperature Atomic Layer Deposited Electron Transport Layers for Coâ€Evaporated Perovskite Solar Cells. Solar Rrl, 2022, 6, 2100842.	5.8	16

#	Article	IF	CITATIONS
217	Novel Zn–Sn–O nanocactus with excellent transport properties as photoanode material for high performance dye-sensitized solar cells. Nanoscale, 2011, 3, 4640.	5.6	15
218	Modulating the optical and electrical properties of all metal oxide solar cells through nanostructuring and ultrathin interfacial layers. Electrochimica Acta, 2012, 85, 486-491.	5.2	15
219	Enhanced Coverage of Allâ€Inorganic Perovskite CsPbBr ₃ through Sequential Deposition for Green Lightâ€Emitting Diodes. Energy Technology, 2017, 5, 1859-1865.	3.8	15
220	One-Pot Synthesis and Structural Evolution of Colloidal Cesium Lead Halide–Lead Sulfide Heterostructure Nanocrystals for Optoelectronic Applications. Journal of Physical Chemistry Letters, 2021, 12, 9569-9578.	4.6	15
221	Tailoring the EnergyÂManifold of Quasiâ€Twoâ€Dimensional Perovskites for Efficient Carrier Extraction. Advanced Energy Materials, 2022, 12, .	19.5	15
222	Defect Passivation Using a Phosphonic Acid Surface Modifier for Efficient RP Perovskite Blue-Light-Emitting Diodes. ACS Applied Materials & Interfaces, 2022, 14, 34238-34246.	8.0	15
223	Decoupling light absorption and charge transport properties in near IR-sensitized Fe2O3 regenerative cells. Energy and Environmental Science, 2013, 6, 3280.	30.8	14
224	Disordered Polymer Antireflective Coating for Improved Perovskite Photovoltaics. ACS Photonics, 2020, 7, 1971-1977.	6.6	14
225	Efficient and stable planar perovskite solar cells using co-doped tin oxide as the electron transport layer. Journal of Power Sources, 2020, 471, 228443.	7.8	14
226	Molecular Engineering of Pure 2D Leadâ€lodide Perovskite Solar Absorbers Displaying Reduced Band Gaps and Dielectric Confinement. ChemSusChem, 2020, 13, 2693-2701.	6.8	14
227	Inorganic electrochromic transistors as environmentally adaptable photodetectors. Nano Energy, 2022, 97, 107142.	16.0	14
228	Fabrication of Unipolar Graphene Field-Effect Transistors by Modifying Source and Drain Electrode Interfaces with Zinc Porphyrin. ACS Applied Materials & Interfaces, 2012, 4, 1434-1439.	8.0	13
229	Direct measurement of coherent phonon dynamics in solution-processed stibnite thin films. Physical Review B, 2014, 90, .	3.2	13
230	Grain Size Modulation and Interfacial Engineering of CH ₃ NH ₃ PbBr ₃ Emitter Films through Incorporation of Tetraethylammonium Bromide. ChemPhysChem, 2018, 19, 1075-1080.	2.1	13
231	Fourâ€Terminal Perovskite on Silicon Tandem Solar Cells Optimal Measurement Schemes. Energy Technology, 2020, 8, 1901267.	3.8	13
232	Interlayer Engineering for Flexible Large-Area Planar Perovskite Solar Cells. ACS Applied Energy Materials, 2020, 3, 777-784.	5.1	13
233	Enhanced Efficiency of Dye-Sensitized Solar Cells with Mesoporous–Macroporous TiO2 Photoanode Obtained Using ZnO Template. Journal of Electronic Materials, 2017, 46, 3801-3807.	2.2	12
234	Modulating Excitonic Recombination Effects through Oneâ€Step Synthesis of Perovskite Nanoparticles for Lightâ€Emitting Diodes. ChemSusChem, 2017, 10, 3818-3824.	6.8	12

#	Article	IF	CITATIONS
235	Perovskite templating <i>via</i> a bathophenanthroline additive for efficient light-emitting devices. Journal of Materials Chemistry C, 2018, 6, 2295-2302.	5.5	12
236	Highly Efficient Perovskite Solar Cells with Ba(OH) ₂ Interface Modification of Mesoporous TiO ₂ Electron Transport Layer. ACS Applied Energy Materials, 2018, 1, 5847-5852.	5.1	12
237	Bistable Amphoteric Native Defect Model of Perovskite Photovoltaics. Journal of Physical Chemistry Letters, 2018, 9, 3878-3885.	4.6	12
238	Cesium Oleate Passivation for Stable Perovskite Photovoltaics. ACS Applied Materials & Interfaces, 2019, 11, 27882-27889.	8.0	12
239	Perturbation-Induced Seeding and Crystallization of Hybrid Perovskites over Surface-Modified Substrates for Optoelectronic Devices. ACS Applied Materials & Interfaces, 2019, 11, 27727-27734.	8.0	12
240	Solution processable nanoparticles as high-k dielectric for organic field effect transistors. Organic Electronics, 2010, 11, 1660-1667.	2.6	11
241	Evolution of Charge Collection â^• Separation Efficiencies in Dye-Sensitized Solar Cells Upon Aging: A Case Study. Journal of the Electrochemical Society, 2011, 158, B1158.	2.9	11
242	Influence of size and shape of sub-micrometer light scattering centers in ZnO-assisted TiO 2 photoanode for dye-sensitized solar cells. Physica B: Condensed Matter, 2018, 532, 225-229.	2.7	11
243	Inducing Isotropic Growth in Multidimensional Cesium Lead Halide Perovskite Nanocrystals. ChemPlusChem, 2018, 83, 514-520.	2.8	11
244	Fieldâ€Ðriven Athermal Activation of Amorphous Metal Oxide Semiconductors for Flexible Programmable Logic Circuits and Neuromorphic Electronics. Small, 2019, 15, e1901457.	10.0	11
245	Inducing thermoreversible optical transitions in urethane-acrylate systems <i>via</i> ionic liquid incorporation for stretchable smart devices. Journal of Materials Chemistry A, 2021, 9, 13615-13624.	10.3	11
246	Patterned 3-dimensional metal grid electrodes as alternative electron collectors in dye-sensitized solar cells. Physical Chemistry Chemical Physics, 2011, 13, 19314.	2.8	10
247	Improved electrical property of Sb-doped SnO2 nanonets as measured by contact and non-contact approaches. RSC Advances, 2012, 2, 9590.	3.6	10
248	Synthesis, characterization and electrical properties of hybrid Zn2GeO4–ZnO beaded nanowire arrays. Journal of Crystal Growth, 2012, 346, 32-39.	1.5	10
249	MODULATING CH ₃ NH ₃ PbI ₃ PEROVSKITE CRYSTALLIZATION BEHAVIOR THROUGH PRECURSOR CONCENTRATION. Nano, 2014, 09, 1440003.	1.0	10
250	Modulating light propagation in ZnO–Cu2O-inverse opal solar cells for enhanced photocurrents. Physical Chemistry Chemical Physics, 2015, 17, 21694-21701.	2.8	9
251	Charge Transport in Organometal Halide Perovskites. , 2016, , 201-222.		9
252	Potassium Acetate-Based Treatment for Thermally Co-Evaporated Perovskite Solar Cells. Coatings, 2020, 10, 1163.	2.6	9

#	Article	IF	CITATIONS
253	Enhanced stability and photovoltaic performance of planar perovskite solar cells through anilinium thiobenzoate interfacial engineering. Journal of Power Sources, 2020, 479, 228811.	7.8	9
254	Suppressing the δ-Phase and Photoinstability through a Hypophosphorous Acid Additive in Carbon-Based Mixed-Cation Perovskite Solar Cells. Journal of Physical Chemistry C, 2021, 125, 6585-6592.	3.1	9
255	Enhanced Thermal Stability of Planar Perovskite Solar Cells Through Triphenylphosphine Interface Passivation. ChemSusChem, 2022, , .	6.8	9
256	Acetic acid effects on enhancement of growth rate and reduction of amorphous carbon deposition on CNT arrays along a growth window in a floating catalyst reactor. Applied Physics A: Materials Science and Processing, 2009, 97, 417-424.	2.3	8
257	Determining the Conductivities of the Two Charge Transport Phases in Solid-State Dye-Sensitized Solar Cells by Impedance Spectroscopy. Journal of Physical Chemistry C, 2013, 117, 10980-10989.	3.1	8
258	Carrier cascade: Enabling high performance perovskite light-emitting diodes (PeLEDs). Current Opinion in Electrochemistry, 2018, 11, 91-97.	4.8	8
259	Toward Efficient and Stable Perovskite Photovoltaics with Fluorinated Phosphonate Salt Surface Passivation. ACS Applied Energy Materials, 2021, 4, 2716-2723.	5.1	8
260	Efficient bandgap widening in co-evaporated MAPbI ₃ perovskite. Sustainable Energy and Fuels, 2022, 6, 2428-2438.	4.9	8
261	Interfacial passivation with 4-chlorobenzene sulfonyl chloride for stable and efficient planar perovskite solar cells. Journal of Materials Chemistry C, 2022, 10, 9044-9051.	5.5	8
262	Heterogeneous electron transporting layer for reproducible, efficient and stable planar perovskite solar cells. Journal of Power Sources, 2019, 437, 226907.	7.8	7
263	Forming-Less Compliance-Free Multistate Memristors as Synaptic Connections for Brain-Inspired Computing. ACS Applied Electronic Materials, 2020, 2, 817-826.	4.3	7
264	Metal Coordination Sphere Deformation Induced Highly Stokesâ€6hifted, Ultra Broadband Emission in 2D Hybrid Leadâ€Bromide Perovskites and Investigation of Its Origin. Angewandte Chemie, 2020, 132, 10883-10888.	2.0	7
265	Synthesis of bismuth sulphoiodide thin films from single precursor solution. Solar Energy, 2021, 230, 714-720.	6.1	7
266	Optimal Shell Thickness of Metal@Insulator Nanoparticles for Net Enhancement of Photogenerated Polarons in P3HT Films. ACS Applied Materials & Interfaces, 2016, 8, 2464-2469.	8.0	6
267	Precursor non-stoichiometry to enable improved CH ₃ NH ₃ PbBr ₃ nanocrystal LED performance. Physical Chemistry Chemical Physics, 2018, 20, 5918-5925.	2.8	6
268	Regulating Vertical Domain Distribution in Ruddlesden–Popper Perovskites for Electroluminescence Devices. Journal of Physical Chemistry Letters, 2019, 10, 7949-7955.	4.6	5
269	Effects of Allâ€Organic Interlayer Surface Modifiers on the Efficiency and Stability of Perovskite Solar Cells. ChemSusChem, 2021, 14, 1524-1533.	6.8	5
270	Advances and Potentials of NiO _{<i>x</i>} Surface Treatments for pâ^'iâ^'n Perovskite Solar Cells. Solar Rrl, 2022, 6, .	5.8	5

#	Article	IF	CITATIONS
271	Optically Pumped Distributed Feedback Laser from Organo-Lead Iodide Perovskite Thin Films. , 2015, , .		4
272	Solution grown double heterostructure on a large hybrid halide perovskite crystal. CrystEngComm, 2018, 20, 6653-6661.	2.6	4
273	A Microfabricated Dual Slip-Pressure Sensor with Compliant Polymer-Liquid Metal Nanocomposite for Robotic Manipulation. Soft Robotics, 2022, 9, 509-517.	8.0	4
274	MXene incorporated polymeric hybrids for stiffness modulation in printed adaptive surfaces. Nano Energy, 2021, 90, 106548.	16.0	4
275	Cu-S Nanocabbage Films with Tunable Optical Bandgap and Substantially Improved Stability by Pulse Electrodeposition. Journal of the Electrochemical Society, 2011, 158, E60.	2.9	3
276	Energy band and optical modeling of charge transport mechanism and photo-distribution of MoO3/Al-doped MoO3 in organic tandem cells. Functional Materials Letters, 2020, 13, 2051003.	1.2	3
277	Bilayer BaSnO ₃ thin film transistors on silicon substrates. Journal of Materials Chemistry C, 2020, 8, 5231-5238.	5.5	3
278	Advances in Perovskite Optoelectronics: Bridging the Gap Between Laboratory and Fabrication. Advanced Energy Materials, 2020, 10, 2000393.	19.5	3
279	Molecular design of two-dimensional perovskite cations for efficient energy cascade in perovskite light-emitting diodes. Applied Physics Letters, 2021, 119, 154101.	3.3	3
280	Dye-Sensitized Solar Cells Based on Tin Oxide Nanowire Networks. Nanoscience and Nanotechnology Letters, 2012, 4, 733-737.	0.4	2
281	Effect of Nitric Acid Concentration on Doping of Thin Film Single-walled Carbon Nanotubes for Electrode Application in Transparent, Flexible Dye Sensitized Solar Cells. Materials Research Society Symposia Proceedings, 2013, 1436, 57.	0.1	2
282	Top Down Scale-Up of Semiconducting Nanostructures for Large Area Electronics. Journal of Display Technology, 2014, 10, 660-665.	1.2	2
283	Ag nanoparticle-blended plasmonic organic solar cells: performance enhancement or detraction?. , 2014, , .		2
284	Quantifying the Usefulness of Oxide-Encapsulated Silver Nanoparticles in Semiconducting Films. Plasmonics, 2017, 12, 1673-1683.	3.4	2
285	Small-area Passivated Contact monoPoly TM Silicon Solar Cells for Tandem Device Integration. , 2019, , .		2
286	Interfacial 2-hydrozybenzophenone passivation for highly efficient and stable perovskite solar cells. Journal of Power Sources, 2020, 475, 228665.	7.8	2
287	Tunable Electroluminescence for Pure White Emission From a Perovskiteâ€Based LED. Advanced Electronic Materials, 2021, 7, 2001227.	5.1	2
288	Oligothiophenes bearing polar groups for organic thin film transistors: synthesis, characterisation and preliminary gas sensing results. , 2007, , .		1

#	Article	IF	CITATIONS
289	Photovoltaics: Temperature and Electrical Poling Effects on Ionic Motion in MAPbI ₃ Photovoltaic Cells (Adv. Energy Mater. 18/2017). Advanced Energy Materials, 2017, 7, .	19.5	1
290	Electromigration of lower and upper Cu lines in dual-damascene Cu interconnects. Materials Research Society Symposia Proceedings, 2003, 766, 3131.	0.1	1
291	Large-area, flexible, integrable and transparent DEAs for haptics. , 2019, , .		1
292	Olivine-Carbon Nanofibrous Cathodes for Lithium Ion Batteries. Materials Research Society Symposia Proceedings, 2010, 1266, 50201.	0.1	0
293	Modification of Electronic Properties of Graphene with Porphyrin Self-Assembled Monolayers and Photoinduced Interactions. Nanoscience and Nanotechnology Letters, 2012, 4, 743-746.	0.4	0
294	Carrier dynamics in low-dimensional perovskites. , 2016, , .		0
295	Surface texture change on-demand and microfluidic devices based on thickness mode actuation of dielectric elastomer actuators (DEAs). , 2017, , .		Ο
296	Plasmonic Entities within the Charge Transporting Layer. SpringerBriefs in Applied Sciences and Technology, 2017, , 47-80.	0.4	0
297	Coâ€Evaporated MAPbI ₃ : Excellent Intrinsic Longâ€Term Thermal Stability of Coâ€Evaporated MAPbI ₃ Solar Cells at 85 °C (Adv. Funct. Mater. 22/2021). Advanced Functional Materials, 2021, 31, 2170155.	14.9	0
298	Exciton Delocalization Across the Organic Spacer: Origin of Ultrafast Energy Funnelling in Ruddlesden-Popper Perovskites. , 0, , .		0
299	Hot Carrier Temperatures in Halide Perovskites: A Closer Look. , 0, , .		0
300	The Effect of Annealing Temperature on the Optical Properties of In ₂ S ₃ Thin Film. Nanoscience and Nanotechnology Letters, 2012, 4, 747-749.	0.4	0
301	Metal-Halide Perovskite Nanocrystals: Unlocking Size Dependent Effects for High Performance Solar Cells and Light-Emitting Devices. , 0, , .		0
302	Large Area Perovskite Solar Cells and Mini-Modules by Thermal Co-Evaporation. , 0, , .		0
303	Thermally Co-Evaporated Large Area Perovskite Solar Cells and Mini-Modules for tandem integration. , 0, , .		0
304	Reversible photochromism in 110 oriented layered halide perovskite. , 0, , .		0
305	Additives in Halide Perovskite for Blue-LightEmitting Diodes: Passivating Agents or Crystallization Modulators?. , 0, , .		0
306	White Electroluminescence from Perovskite–Organic Heterojunction. , 0, , .		0

#	Article	IF	CITATIONS
307	Inorganic framework of low-dimensional perovskites dictate the performance and stability of mixed-dimensional perovskite solar cells. , 0, , .		0
308	Low dimensional organic metal-halide hybrids: molecular design & optoelectronic properties. , 0, ,		0
309	Ionic, opto-electronic properties of halide perovskites for neuromorphic applications. , 0, , .		0
310	Upcycling Silicon Photovoltaic Waste into Thermoelectrics (Adv. Mater. 19/2022). Advanced Materials, 2022, 34, .	21.0	0